NANO LETTERS

2007
Vol. 7, No. 3
703−706

# Local Electrical Detection of Single Nanoparticle Plasmon Resonance

**Iwijn De Vlaminck,*,† Pol Van Dorpe, Liesbet Lagae, and Gustaaf Borghs**

*Imec, Kapeldreef 75, 3001 Leuven, Belgium*

*Received December 7, 2006; Revised Manuscript Received February 3, 2007*

**ABSTRACT**

**We developed a technique for the local electrical detection of a plasmon resonance in a single metal nanoparticle. A gold nanoparticle is coupled to a GaAs photodetector placed in the particle's near field. Light scattered by the particle is coupled into the semiconductor cavity of the photodetector, providing efficient transduction. Strong multipolar resonances were recorded in the 650–920 nm wavelength range. This local detection technique allows the construction of sensitive nanoscale bioprobes and arrays thereof.**

Surface plasmons are electromagnetic oscillations mediated by charge oscillations; they occur at the surface of noble metals and in noble metal nanoparticles with resonance frequencies in the visible and IR spectrum. The properties of surface plasmons have received great interest in recent years, as it is recognized that they have the ability to overcome the size mismatch between diffraction-limited optical components and nanoscale objects, opening up new possibilities in, e.g., optical signal processing and biosensing. Indeed, it was shown that surface-plasmon-mediated electromagnetic waveguiding is feasible in subwavelength metallic wires or chains of metal nanoparticles,[1] as was predicted earlier.[2,3] Furthermore, efficient modal coupling between plasmon waveguides and dielectric waveguides was demonstrated.[4]

In biosensing, the importance of plasmonics relies in high optical energy confinement and strong local enhancement of electric fields. Biorecognition is achieved in localized surface plasmon resonance (LSPR) biosensors[5,6] through the detection of LSPR spectral changes caused by adsorbate-induced changes in local dielectric constant. Usually, the LSPR spectrum of a nanoparticle surface is studied with an optical detector in the far field.

In this paper, we develop a technique for the local electrical transduction of a plasmon resonance in a single metal nanostructure. We record the optical response of a single metal nanoparticle by means of a nanoscale photodetector placed in the structure's near field. It is well-known that enhanced light absorption in inorganic and organic photodetectors decorated with nanoparticles can be achieved.[7,8] The ability of detecting the plasmon resonance of individual structures leads to enhanced system sensitivity and lowered detection limits in biosensing.[9] It was predicted that single-particle detection techniques could lead to single-molecule detection capabilities for large bioanalytes and that zeptomole limits are within reach for small biomolecules.[9] Local electrical signal transduction has the added advantage that it offers the possibility of constructing bioassays that exploit large-scale parallelism and multiplexing, allowing more information to be extracted from one sample at a time. Furthermore, the construction of fully integrated bioprobes becomes possible with such a technique.[10] The present work may also aid in the development of components for optical-to-electrical signal transduction, useful in photonic circuitry.

The optical detector is a semiconducting photoresistor, the particle is fabricated directly on top of the detector. A reference detector with identical dimensions but without metal particle is constructed nearby (12.5 $\mu$m). Through comparison of the responses of the reference detector and particle-enhanced detector, we are able to discern particle-related spectral features from features related to the wavelength specificity of the photodetector and wavelength-dependent properties of the various components in the measurement setup. An oxide layer between the particle and semiconductor serves as electrical isolation but also allows tuning of the optical response.[11] The photodetectors are made freestanding; as a result, parasitic current paths are avoided, the optical response is tuned, and particle-to-detector light coupling is enhanced due to an increase in optical index contrast.[12]

Layer structures for the optical detector are defined by means of molecular beam epitaxy on GaAs semi-insulating substrates. The active layer, 100 nm *n*-GaAs (2 $e^{18}$ $cm^{-3}$), is grown on a 560 nm sacrificial $Al_{80}Ga_{20}As$ layer. In Figure 1a−c, the fabrication scheme, is outlined. Electron beam

* Corresponding author. E-mail: Iwijn.devlaminck@imec.be. Telephone: +32 16 28 1529.
† Also at Esat-Insys, KULEUVEN, Belgium.

10.1021/nl062861x CCC: $37.00 
**Published on Web 02/22/2007**

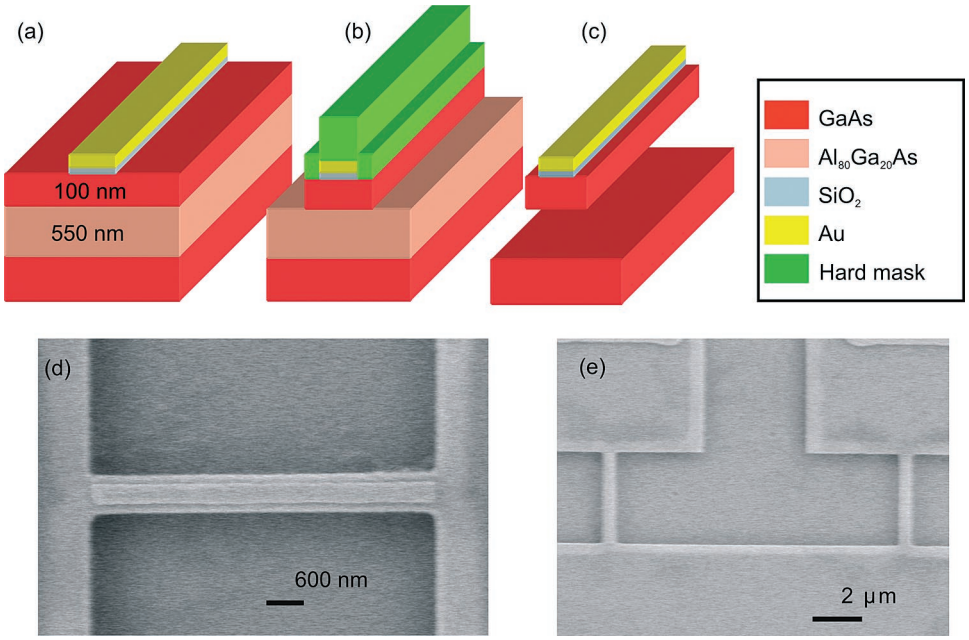


**Figure 1.** (a−d) Fabrication sequence for the gold structure coupled to a semiconducting photodetector. (a) EBL and lift-off for definition Au−$SiO_2$ structure. (b) Second e-beam EBL, definition hard mask, dry etch of GaAs. (c) HF-based selective etch of $Al_{80}Ga_{20}As$, resulting in a freestanding GaAs detector. (d) Scanning electron micrographs of a fabricated structure, width GaAs detector 600 nm, Au structure dimensions: 0.3 $\mu$m × 5 $\mu$m × 0.03 $\mu$m. In panel (e), the detectors with and without particle are shown.

lithography (EBL) is used to define a pattern in a PMMA−PMMA/MA resist layer. A 10 nm $SiO_2$ layer is deposited by sputtering; subsequently, a 30 nm layer of Au is evaporated and the layer structure is transferred with lift-off. After a second EBL step, a hard mask (Ge/Ti 50/50 nm) is made by means of evaporation and lift-off. The pattern is than transferred in the GaAs layer through reactive ion etching in a Cl−Ar plasma. After the subsequent, HF-based underetching of the devices (selective $Al_{80}Ga_{20}As$ etch) and rinsing with $H_2O$, acetone, and isopropyl alcohol, the hard mask is removed. In the last step, ohmic contacts (AuGe/Ni/Au, 120/15/60 nm) are defined with optical lithography evaporation and lift-off. In Figure 1d−e, a scanning electron micrograph (SEM) image of a finished device is shown. Panel (e) shows the detector with particle and the reference detector without such a particle.

The semiconductor cavity on which the metal structure is fabricated significantly influences the structure's response. The polarizability of the substrate gives rise to anisotropic behavior and significant changes in resonance frequency and bandwidth. The influence of the substrate is usually modeled by considering electromagnetic coupling with the image charges induced in the substrate.[13] The substrate-induced inhomogeneity of the local electric field gives rise to efficient coupling of the applied fields to multipole responses of the metal structure.[14] The nonspherical nature of the metal structure makes them particular susceptible to multipolar excitations.[15] Nanostructuring of the dielectric leads to waveguide and cavity effects. The coupling of dipole scatterers to waveguide modes has been calculated, and it was shown that highly efficient coupling can be achieved in case of a high-index contrast of the waveguide system.[12] Furthermore, the semiconductor provides additional channels for energy dissipation, broadening the plasmon response.

To study the optical response of the particle−semiconductor cavity system subject to an incident electromagnetic wave, we employ a two-dimensional (2D) finite difference time-domain (FDTD) method.[16] Experimental data on the frequency-dependent dielectric constants of Au, $SiO_2$, and GaAs, including real and imaginary parts, are fitted and used in the model. The frequency-dependent absorption in the GaAs detector layer is extracted by monitoring the optical power flowing in and out of the semiconductor volume. Results for a model of a semiconductor structure with a particle attached to it are compared to results for a model of an identical semiconductor structure without particle. The simulation area was 1.5 $\mu$m × 1.2 $\mu$m large with perfectly matched layer (PML) type boundaries. After a convergence analysis, a grid size of 2 nm × 2 nm was chosen.

In Figure 2a, the 2D modeled geometry of a semiconductor structure with a particle attached to it is shown. Figure 2b shows the spectrum of absorption in the GaAs layer with particle ($P_1$) compared to the case of a GaAs structure without such a particle ($P_2$). The absorption enhancement spectrum ($P_1/P_2$) shows clear resonance behavior, and the mode-energy is strongly dependent on the width ($w$) of the gold structure. The resonance wavelength of the metal structures scales linearly with the metal−semiconductor cavity size, offering wide-range tunability. The bandwidth of the resonance increases for higher resonance energy, indicating that the semiconductor quenches the plasmon when the absorption in the semiconductor is high, as described elsewhere by Nolte.[17] In Figure 2c, the electrical field intensity distribution of a structure with $w$ = 400 nm is plotted for an off-resonant

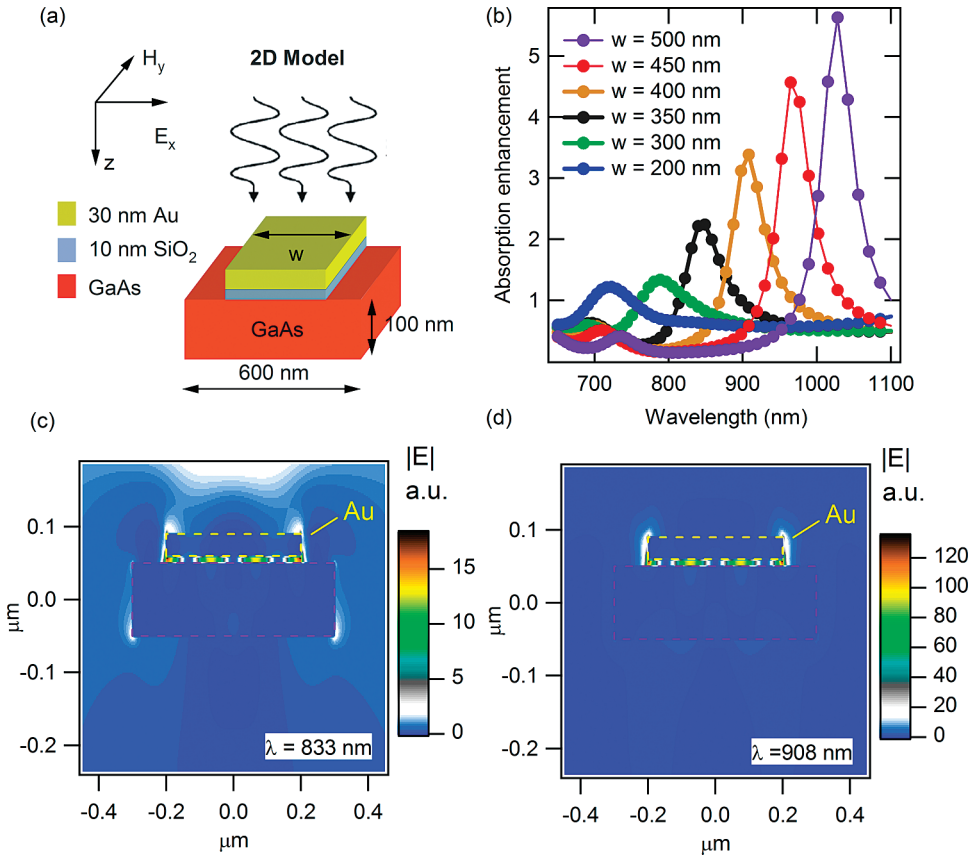


**Figure 2.** (a) Geometry of the modeled device. (b) Response of the particle−semiconductor system compared to the response of photodetector without particle. The spectra show resonance peaks, the resonance wavelength depends on the width of the Au structure. Electrical field intensity for a device with a 400 nm width at (c) $\lambda = 833$ nm and (d) $\lambda = 908$ nm.

excitation wavelength of 833 nm. In Figure 2d, the distribution is shown for an excitation at resonance at 908 nm. In the latter case, the electrical fields are strongly amplified. It is evident from Figure 2c and d that the largest electrical fields are developed across the $SiO_2$ layer, which serves as a spacer layer for the charges in the gold structure and their respective image charges in the GaAs. The occurrence of four spots with high electric field intensity indicates that a multipole is excited. The plasmon-enhanced electrical fields in the GaAs layer lead to enhanced light absorption. Similar calculations show that the dipole modes of the metal−dielectric cavity can be excited in the wavelength range 1250−1800 nm for the same structures.

The experimental setup for spectral analysis is described in Figure 3a. Light from a 300 W Xe lamp is passed through a monochromator (MC) for wavelength selection and is subsequently linearly polarized (P), modulated with an optical chopper (C), and focused on the sample with a lens (L). The electrical configuration is outlined in Figure 3b. A device with a particle and a reference device without a particle are measured simultaneously, a current of 0.2 mA is applied, and the amplitude modulations (rms) in electrical response, $\Delta V_1$ and $\Delta V_2$, respectively, are measured with a lock-in detector. All devices have a resistance of 3.5−4.5 kΩ. Figure 3c shows the frequency response of the lock-in signal of the photodetector with a particle and without a particle. The spectra contain features from the lamp spectrum, the grating spectrum, and the wavelength-dependent absorption characteristics of the GaAs detector. The signal enhancement, $\Delta V_1/\Delta V_2$, for devices with $w = 230$, 270, 310, 350, and 400 nm are shown in Figure 4d. All gold structures have a length of 5 $\mu$m, and the width of the GaAs photodetector is 600 nm. The dimensions of the devices are evaluated with SEM, and the thickness of the Au and $SiO_2$, 30 and 10 nm, are evaluated by means of atomic force microscopy (AFM). The predicted response (Figure 2b) is reproduced; in the inset, the calculated and measured resonance frequencies are plotted and compared. The strongly reduced absorption efficiency for GaAs at energies lower than the band gap energy at room temperature, resulting in a strongly reduced signal for both detectors, restrains the upper limit of the measurement window to 920 nm. An excellent signal-to-noise ratio, however, can be reached at energies higher than the band gap, with a large optical spot size (>1 $mm^2$) and at limited optical input power, indicating the scalability of the technique toward smaller metal structures and indicating the possibility of studying arrays of devices.

In conclusion, we propose a technique for the local transduction of a plasmon resonance in a single metal nanostructure by means of an optical detector fabricated in the particle's near field. The response of the particle−photodetector system was calculated by means of a FDTD method and compared with experimental results. The dependence of the response on the width of the gold particle

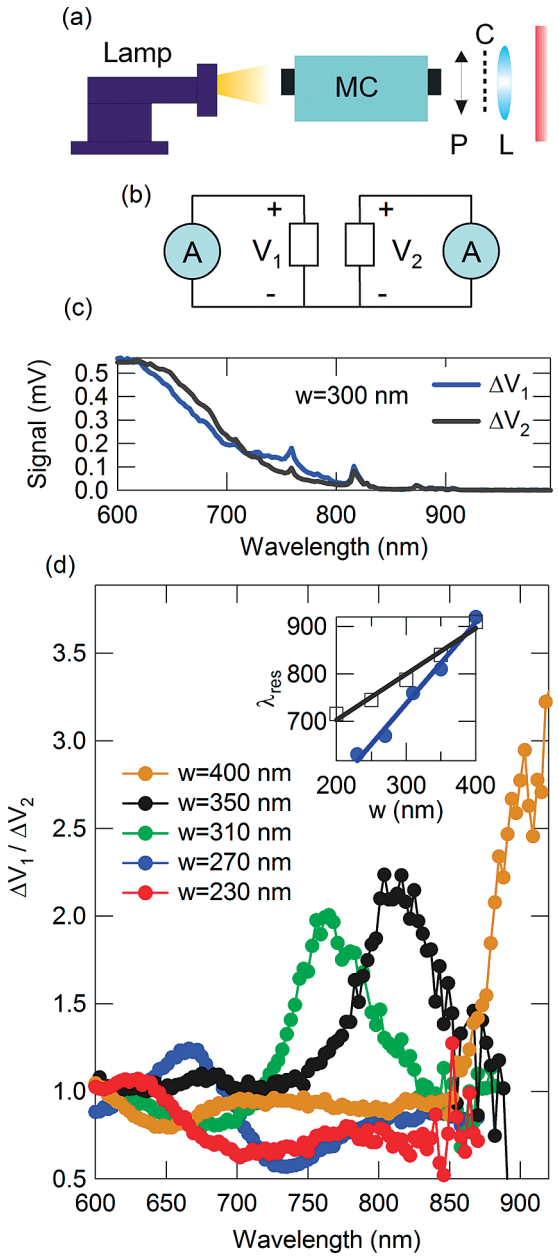


**Figure 3.** (a) Sketch of the measurement setup: light from a xenon lamp is spectrally decomposed with a monochromator, linearly polarized (P), modulated (Chopper C), and focused on the sample. (b) Electrical scheme: a constant current, 0.2 mA, is applied on the detectors with and without particle. The relative response ($\Delta V_1/\Delta V_2$) is recorded with a lock-in amplification technique. (c) Measured response for a detector with ($\Delta V_2$) and without particle ($\Delta V_1$), $w = 300$ nm. In panel (d), the measured response for devices with $w = 230$, 270, 310, 350, and 400 nm are shown. In the inset, the measured (●) and simulated (□) resonant colors ($\lambda_{res}$) as function of $w$ are plotted and compared.

was analyzed. Good agreement between experimental and modeling results was obtained. We believe these results are important for application in biosensing and for optical signal processing. Furthermore, we believe this work shows prospects for the design of plasmon-enhanced photodetectors. Recently, it was proposed that plasmonic antenna structures can be employed in the design of fast and low-noise optical sensors with enhanced response in the IR spectrum.[18,19] In future work, we will focus on scaling structures and optimizing systems for maximized sensitivity. Lower band gap semiconductors can be used as photoactive material to enlarge the spectrum measurable; this should allow us to measure dipole resonances in the 1100−1800 nm wavelength window. Furthermore, the use of biocompatible substrate materials will be investigated.

**Acknowledgment.** We thank Jos Moonens and Hans Costermans for e-beam assistance, Johan Feyaerts and Erwin Vandenplas for technical support, Willem Vandegraaf and Stefan Degroote for MBE growth, David Cheyns for assistance with the measurement setup and discussions, Johan Reynaert, and Maarten Debucquoy for assistance with the measurement setup. I.D.V. acknowledges financial support from the I.W.T. (Flanders), P.V.D. acknowledges financial support from the F.W.O. (Flanders).

## References

(1) Maier, S. A.; Kik, P. G.; Atwater, H. A.; Meltzer, S.; Harel, E.; Koel, B. E.; Requicha, A. A. G. *Nat. Mater.* **2003**, *2*, 229.
(2) Quinten, M.; Leitner, A.; Krenn, J. R.; Aussenegg, F. R. *Opt. Lett.* **1998,** *23*, 1331.
(3) Takahara, J.; Yamagishi, S.; Taki, H.; Morimoto, A.; Kobayashi, T. *Opt. Lett.* **1997**, *22*, 475.
(4) Hochberg, M.; Baehr-Jones, T.; Walker, C.; Scherer, A. *Opt. Express* **2004,** *12*, 5481.
(5) Haes, A. J.; Van Duyne, R. P. *Anal. Bioanal. Chem.* **2004**, *379*, 920.
(6) Frederix, F.; Friedt, J.-M.; Choi, K.-H.; Laureyn, W.; Campitelli, A.; Mondelaers, D.; Maes, G.; Borghs, G. *Anal. Chem.* **2003**, *75*, 6894.
(7) Stuart, H. R.; Hall, D. G. *Appl. Phys. Lett.* **1996**, *69*, 2327.
(8) Rand, B. P.; Peumans, P.; Forrest, S. R. *J. Appl. Phys.* **2004**, *96*, 7519.
(9) McFarland, A. D.; Van Duyne, R. P. *Nano Lett.* **2003**, *3*, 1057.
(10) Alivisatos, P. *Nat. Biotech.* **2004,** *22*, 47.
(11) Su, K. H.; Wei, Q. H.; Zhang, X. *Appl. Phys. Lett.* **2006,** *88*, 063118.
(12) Soller, B. J.; Stuart, H. R.; Hall, D. G. *Opt. Lett.* **2001,** *26*, 1421.
(13) Pinchuk, A.; Hilger, A.; von Plessen, G.; Kreibig, U. *Nanotechnology* **2004,** *15*, 1890.
(14) Khlebtsov, B.; Melnikov, A.; Zharov, V.; Khlebtsov, N. *Nanotechnology* **2006**, *17*, 1437.
(15) Krenn, J. R.; Schider, G.; Rechberger, W.; Lamprecht, B.; Leitner, A.; Aussenegg, F. R.; Weeber, J. C. *Appl. Phys. Lett.* **2000**, *77*, 3379.
(16) www.lumerical.com/fdtd.
(17) Nolte, D. D. *J. Appl. Phys.* **1994**, *76*, 3740.
(18) Ishi, T.; Fujikata, J.; Makita, K.; Baba, T.; Ohashi, K. *Jpn. J. Appl. Phys.* **2005**, *44*, L364.
(19) Yu, Z.; Veronis, G.; Fan, S.; Brongersma, M. L. *Appl. Phys. Lett.* **2006**, *89*, 151116.

NL062861X